UCRL-11321
c.2

University of California

Ernest O. Lawrence Radiation Laboratory

TWO-WEEK LOAN COPY

This is a Library Circulating Copy which may be borrowed for two weeks. For a personal retention copy, call Tech. Info. Division, Ext. 5545

SEMIAUTOMATIC SCANNING OF PROTON-RECOIL TRACKS IN NUCLEAR EMULSION

Berkeley, California

UCRL-11321
c.2

DISCLAIMER

This document was prepared as an account of work sponsored by the United States Government. While this document is believed to contain correct information, neither the United States Government nor any agency thereof, nor the Regents of the University of California, nor any of their employees, makes any warranty, express or implied, or assumes any legal responsibility for the accuracy, completeness, or usefulness of any information, apparatus, product, or process disclosed, or represents that its use would not infringe privately owned rights. Reference herein to any specific commercial product, process, or service by its trade name, trademark, manufacturer, or otherwise, does not necessarily constitute or imply its endorsement, recommendation, or favoring by the United States Government or any agency thereof, or the Regents of the University of California. The views and opinions of authors expressed herein do not necessarily state or reflect those of the United States Government or any agency thereof or the Regents of the University of California.

UCRL-11321

For RSI

UNIVERSITY OF CALIFORNIA

Lawrence Radiation Laboratory
Berkeley, California

AEC Contract No. W-7405-eng-48

SEMIAUTOMATIC SCANNING OF PROTON-RECOIL TRACKS IN NUCLEAR EMULSION

Richard L. Lehman and Olga M. Fekula

March 11, 1964

SEMIAUTOMATIC SCANNING OF PROTON-RECOIL TRACKS IN NUCLEAR EMULSION

Richard L. Lehman and Olga M. Fekula

Lawrence Radiation Laboratory
University of California
Berkeley, California

March 11, 1964

ABSTRACT

The sampling bias in proton-recoil track samples selected by a new rapid method from nuclear emulsion has been examined. Track-length distributions of the samples taken from six emulsions exposed to single-energy fast neutrons are compared to those predicted by an equation derived for this purpose. Bias in the angular distribution of the sampled tracks was similarly examined. The types and sources of tracks, and neutron scattering in the emulsion, are discussed.

The energy of the neutron beams was determined separately by two methods: differentiation of the proton-track energy distribution, and direct measurement of track length and scattering angle. The former yielded more precise values.

An operational description of equipment used for semiautomatic track scanning is given.

SEMIAUTOMATIC SCANNING OF PROTON-RECOIL TRACKS IN NUCLEAR EMULSION

Richard L. Lehman* and Olga M. Fekula

Lawrence Radiation Laboratory
University of California
Berkeley, California

March 11, 1964

I. INTRODUCTION

The development of microscopes adapted for automatic coordinate readout has increased the potential usefulness of nuclear track emulsion as a fast-neutron spectrometer.[1,2] The analysis of a proton-recoil track sample can reveal the fast-neutron energy spectrum to which the emulsion has been exposed.[3] However, although automatic readout solved the problem of rapid recording of track measurements (see Appendix), it did not solve the central problem in this use of nuclear track emulsion, that of rapid unbiased track sampling.

The standard sampling method of measuring the length of every track within a given volume of emulsion is too slow: it cannot match the speed of the recording system. Because of this, the more rapid random-walk sampling method has been introduced: that track is measured one of whose ends is nearest to the end point of the previous track.[4] Although intuitively one would think that the random-walk method would give an unbiased track sample, it can be argued that because the shorter tracks present effectively only one end point to the scanner, this method biases against them.[5] In an attempt to answer the question, "How much bias, if any, does the random-walk method introduce?"

proton-recoil track distributions taken from nuclear emulsions exposed to single-energy fast neutrons have been compared with those predicted by theory.

II. PROCEDURES

A. Experimental Method

Pellicles of unmounted Ilford L.4 nuclear track emulsion, 1 by 3 in. and 600 μ thick, were wrapped in a single layer of black paper. These were mounted in a special holder (Fig. 1) and exposed, edge-normal, to single-energy neutrons 18 cm from a tritium or deuterium target (and at 0° from the beam axis) at the U. S. Naval Radiological Defense Laboratory Van de Graaff accelerator. In order to minimize neutron scattering, the beam was directed into a tent-walled room outside the accelerator building, where it struck the target located 1.5 m above a cement floor. The fast-neutron intensity was monitored by a BF_3 long counter, 1.0 meter distant from the target and at an angle of 45° from the beam axis. The exposure details are given in Table I.

After the exposures, the films were opened in a darkroom and measured for thickness and lateral extent. They were then developed and fixed by a modified cold-cycle process[4] in which the solutions were kept at 5°C. To reduce thickness shrinkage, the processed emulsions were soaked for 24 hours in a concentrated solution of wood rosin in ethanol (35 g per 100 ml). In this case, the rosin treatment caused a 3 to 10% net permanent swelling of the emulsion over the initial dimensions. The films were mounted on 1X3-in. microslides with clear epoxy cement before they were scanned. The emulsions were manufactured 27 February 1961, developed 3 months later, and scanned within 6 months of development.

The center third of the 1×3-in. emulsions were scanned by the random-walk method until 1000 to 3000 track samples were obtained. This was 0.1 to 0.3% of the approximately 1 million tracks in this sampling volume.

The tracks were analyzed into length and energy spectra by an IBM 650 computer that was directed by the special program RECOIL I.[4] Also, separately, those tracks making a polar half angle of 30 deg or less with the beam axis (that was carefully aligned with the y axis of the nuclear emulsion) were selected by use of a new program, RECOIL II, to recreate the incident neutron spectrum. RECOIL II computed the energy of a neutron by use of

$$E_n = E_p \sec^2 \theta . \qquad (1)$$

The computer obtains the value E_p by comparing the track length ℓ with a range-energy table.[6] The product of this value and $\ell^2/(\Delta y)^2$ gives the neutron energy, which is then sorted into one of 85 intervals. Thus the raw neutron spectrum is generated track by track. At the end of the computation, the number in each interval is corrected by the factor $1/\sigma P \Delta E$. RECOIL II also analyzed the accepted tracks into length intervals, and into angular intervals in the vertical and horizontal planes of the emulsion.

B. Expected Unbiased Sampling Distributions

The basic equation that describes the scattering distributions from single-energy (< 20 MeV) neutron collision with hydrogen nuclei is

$$\frac{dN}{d\Omega^*} = \frac{N_0}{4\pi} \qquad (2)$$

(where * denotes center-of-mass coordinate system),

from which can be derived

$$\frac{dN}{d\Omega} = \frac{N_0}{\pi} \left[1 - \frac{\Omega_0}{2\pi}\right] = \frac{N_0}{\pi} \cos\theta \tag{3}$$

$$\frac{dN}{d\theta} = N_0 \sin 2\theta, \tag{4}$$

and

$$\frac{dN}{dE_p} = \frac{N_0}{E_n} . \tag{5}$$

If it is assumed that

$$\ell = a\, E_p^n , \tag{6}$$

in which a and n are constants so that

$$\ell_m = a\, E_n^n , \tag{7}$$

then one may write

$$\frac{dN}{d\ell} = \frac{N_o}{n} \left(\ell^{(1/n-1)} / \ell_m^{1/n}\right) . \tag{8}$$

The conclusions of this paper are based on a comparison of actual sample distributions with those predicted by Eq. (8). Because the form of this equation is important, it is presented in Fig. 2.

III. EXPERIMENTAL RESULTS

The raw length-distributions of tracks taken by random-walk sampling from nuclear emulsions exposed to single-energy neutrons are presented in Figs. 3 through 8. The length distribution for that fraction of the tracks scattered into a forward cone of half angle of 30 deg is also given for each sample. Details of the track measurements may be seen in Table II.

The 0-to-30-deg fractions have been analyzed into scattering-angle distributions in the xy and zy planes of the emulsion (Figs. 9 through 14). In addition, the energy spectra of the incident neutrons have been re-created from measurements by two different methods. One method uses only the forward 0- to 30-deg fraction (RECOIL II); the other uses the entire proton track sample after it has been converted into an energy distribution (RECOIL I). In the latter case, the neutron spectrum is obtained by differentiation of the energy distribution of the proton tracks.[3] The neutron spectra from both methods are presented for comparison in Figs. 15 through 20.

IV. DISCUSSION

A. Track Length Distribution; Bias

A list of the types and sources of the tracks in the length distributions (Figs. 3 through 8) is helpful in the analysis for sampling bias:

(a) proton tracks from first collisions of the primary neutron beam with hydrogen nuclei, either directly (H), or after one or two previous scatterings from the heavier nuclei in the emulsion (ZH or ZZ'H);

(b) proton tracks from second or third collisions of the neutron beam with hydrogen nuclei (HH', ZHH', or HH'H'');

(c) proton tracks from nuclear n, p reactions;

(d) α-particle tracks from nuclear n, α reactions, and

(e) α-particle tracks from the decay of radioactive contaminants present in the manufactured emulsions (no attempt was made to distinguish between α-particle and proton tracks during the sampling).

The expected length distributions (Eq. 8) are composed exclusively of type (a) tracks, and the distributions of tracks of types (b) through (e) are superimposed on the expected distributions. The relative numbers of tracks of types (a) and (b) may be found by use of Fig. 21, which gives the probabilities for neutron interactions with the various elements in nuclear emulsion.

The fraction of the total number of proton-recoil tracks of type (b) was found to be 0.13, 0.10, 0.09, 0.05, 0.04, and 0.02 respectively, for the distributions in Figs. 3 through 8. These tracks are not easily seen because they form a smooth distribution of relatively short lengths that is superimposed on the basic or type (a) distribution. For the distributions in Figs. 3, 4, and 5, most of these tracks fall in the 7- to 3-μ length region where the sampling efficiency drops to zero. The type (b) tracks are not seen in Figs. 6, 7, and 8 for a different reason: they are relatively few in number, and they are spread out over a wide range of lengths.

Tracks from the two sources that constitute type (a) are separated by use of information from the 30-deg fraction of the total track sample. The ratio of the measured values of $\Delta N/\Delta \ell$ (taken near the maximum track length of the sample) gives the ratio $H/(H + ZH + ZZ'H)$ for tracks of type (a). This is so because a 30-deg fraction track of length ℓ_m must be an H track. The measured ratios 0.70, 0.66, 0.59, 0.89, 0.98, and 1.0, respectively, for the distributions in Figs. 3 through 8 agree to ± 10% with estimates based on the elastic scattering probabilities in Fig. 21.

Although many nuclear (n, p), (n, d), (n, T), (n, He^3), and (n, α) reactions are energetically possible with the heavy nuclei present in nuclear emulsion,[7] only the O (n, α)C and the N(n, α)B reactions generate numbers of tracks that are significant in comparison with the proton recoils. The charts of Howerton[8] were used to compute that the former reaction will generate 8- to 9-μ tracks in film A-21, and 80-μ tracks in film A-23, amounting to respectively 3% and 8% of the expected proton recoils. The latter reaction generates 110-μ tracks in film A-23, amounting to 1% of the proton recoils. The 6- to 7-μ tracks from the N(n, p)C reaction, common when nuclear emulsion is exposed to thermal neutrons, are not in evidence.

The prominent peak near 21 μ in films A-20, A-21, and A-23 is composed of α tracks from decay of radioactive substances present in the emulsion. Although it has been impossible to identify the emitters that contribute to this peak, they may be among the following: Ra^{226}, 19 μ; Rn^{222}, 24 μ; Th^{228}, 23 μ; Ra^{224}(Th X), 25 μ; Ra^{220}(Tn), 29 μ; and Pu^{239}, 21 μ. Small peaks from Po^{214}(Ra C'), 40 μ and Po^{212}(Th C'), 48 μ are indicated by the numbers 2 and 3 in Fig. 8.

Below 200 μ, the measured track distribution of film A-23 departs strongly from that expected. The track evidence indicates that the 15.2-MeV neutron beam was not pure, but was mixed with significant numbers of 2- to 3-MeV neutrons. Such a mixture is not uncommon when tritium targets are bombarded with deuterium: the target may take up deuterium gas and thereby become a mixed tritium-deuterium target. It appears likely that this explanation applies here, and that the 2- to 3-MeV neutrons were generated in a D(d, n)He^3 competing reaction in the target.

B. Angular Sampling Bias in the 30-Degree Fraction

Each track accepted in the 30-deg fraction was analyzed by its inclination in the horizontal (xy) and vertical (zy) planes of the emulsion. The inclinations were sorted into one of 10 intervals between +30° and -30°.

In Figs. 9, 10, and 11, those tracks with small-angle scattering have been equally divided among the four central intervals for a smooth presentation. This was done because of the "quantum" effect of short tracks measured to discrete length intervals (4μ). This effect also gives rise to the undulations that are present at $\sin\theta = 0.25$ and 0.35. Where the track lengths are greater, as in Figs. 12 and 13, the undulations damp out. However, they recur in Fig. 14, where the distribution consists of mixed long and short tracks.

A measuring bias in the zy (depth) plane is evident in all samples; the precise depth inclination is not recorded. There is a uniform tendency of the scanner to underestimate the depth differences between the track end points. This may be due to insufficient care in coming to a sharp depth focus on the terminal grains.

C. The Measured Neutron Spectra

The neutron spectra measured by the differentiation method were in each case more precise than those measured by the secant-squared method (Figs. 15 through 20). This somewhat surprising finding may be explained as follows:

1. The 30-deg samples in all cases contained considerable numbers of tracks shorter than the expected cutoff at $\approx 0.6\,\ell_m$. These consist of high-angle ZH tracks, secondary-scattering HH' and ZHH' tracks, and α-particle tracks. Such tracks give low-energy tails to the neutron spectra.

2. The energy of a single neutron computed by use of the secant-squared method is the product of three measured quantities (see Sec. IIA),

each of which has an associated error. The measurement of slope at the (maximum) energy cutoff is, on the other hand, subject only to the uncertainty in one measured quantity, the track length.

V. CONCLUSIONS

Track samples obtained by the random-walk method have length and angular distributions that agree with those predicted by equations derived from s-wave collision dynamics. The track samples contain, in addition to the expected tracks, significant numbers of tracks from α particles and from second collisions of the neutron beam with hydrogen nuclei.

The determination of the energy of the incident neutrons by differentiation of the proton-track energy distribution may be more precise than the determination by direct measurement of track length and scattering angle.

APPENDIX

Description of a Semiautomatic Track-Scanning Apparatus

The heart of an apparatus that has given three years of trouble-free service at the Lawrence Radiation Laboratory (University of California) is a standard research microscope fitted with a special stage and base (Fig. 22). Two hand dials drive the precision lead screws that control the horizontal (x- and y-axis) motion of the stage. The vertical (z-axis) motion of the microscope barrel is controlled by the standard coarse- and fine-focus knobs.

Shaft-position encoders (Model C-102, Datex Corporation, Monrovia, California) affixed to the special aluminum base plate are mechanically coupled to the precision lead screw shafts and to the shaft of the fine-focus knob. These encoders "sense" minute rotation increments as electrical impulses that can be translated and amplified. The encoders resolve 1000 units/turn or about 0.36 deg of shaft rotation. A special adaptor on the x and y encoders permits a unique digital readout over the range of 100 turns. Suitable gearing and intermediate binary-to-decimal electronic translating (Model K-106, Datex Corporation, Monrovia, California) enable the encoders to read out to a card-punch machine in units of micrometers of translational stage or barrel motion. Thus, at a fixed coarse-focus setting, every point in the working volume has a unique set (x_i, y_i, z_i) of rectangular space coordinates. A point of interest is located by cross hairs in the field of view and by the fine-focus setting.

The electrical-information flow from the shaft-position encoders to the punch-card machine is shown by block diagram in Fig. 23, and a photograph of the entire apparatus appears as Fig. 24. When the scanner pushes the

"punch" button on the control box (Fig. 22), the three shaft-encoder positions are sensed and the output system is activated.

The punch machine is so programmed that columns 1 through 10 in the punch cards are automatically filled with fixed information as each new card is fed into it. The fixed information consists of the date, the relative humidity, and the emulsion number in coded (decimal) form. Normally this information is constant for several hundred cards. It is controlled by 10 switches mounted on the panel shown in Fig. 24. As the end point of a track is located by the cross hairs in the field of view and the "punch" button is pushed, columns 11 through 25 are punched--five columns for the decimal coordinate of each axis. When the other end of the track is located by the scanner and the "punch" button is pushed, columns 26 through 40 are filled with the new end-point coordinates. Similarly columns 41 through 55 and columns 56 through 70 are filled with the end-point coordinates of a second track. When column 70 is punched the card is automatically rejected and a new card is fed into the punch machine, ready for columns 11 through 25 to be filled with the end-point coordinates of a new track.

This system allows a scanner to work rapidly, since he may keep his eyes continuously accommodated to the microscopic field of view. The minimum time required to record both end points of a track is about 2.5 seconds. This does not include the scanning time for locating the end points, however, and in practice the minimum time averaged over an hour of scanning is about 12 sec per track.

*Present address: Department of Biophysics and Nuclear Medicine, University of California, Los Angeles.

1. Walter H. Barkas, Nuclear Research Emulsions (Academic Press, New York, 1963), p. 458 ff.

2. R. L. Lehman, H. Akagi, and O. M. Fekula, Neutron Dosimetry Near a Bare Pulsed Reactor, Health Phys. to be published (UCRL-10907 July 15, 1963).

3. J. H. Roberts, Absolute Flux Measurement of Anisotropic Neutron Spectra with Proton Recoil Tracks in Nuclear Emulsions, Rev. Sci. Instr. 28, 677 (1957).

4. H. Akagi and R. L. Lehman, Neutron Dosimetry by Use of Nuclear Track Emulsion, Health Phys. 9, 207 (1963).

5. William G. Simon, (Lawrence Radiation Laboratory), private communication.

6. Ref. 1, page 438.

7. V. J. Ashley and H. C. Catron, Tables of Nuclear Reaction Q-Values, Lawrence Radiation Laboratory Report UCRL-5419, Feb. 1959 (unpublished).

8. Robert J. Howerton, Semi-Empirical Cross Sections, 0.5-15 MeV, Part II, Lawrence Radiation Laboratory Report UCRL-5351, Nov. 1958 (unpublished).

Table I. Details of neutron exposure.

Film no.	Reaction	Duration (min.)	Beam E (MeV)	Av. beam current (μA)	Neutron E at 0° (MeV)	Neutron exposure at 18 cm 0° (n $cm^{-2} \times 10^{-6}$)
A-15	$T(p,n)He^3$	45	1.44-1.50	6	0.48-0.56	29.5
A-16	$T(p,n)He^3$	15	1.72-1.75	10	0.79-0.85	22.5
A-18	$T(p,n)He^3$	45	1.93-1.95	6.5	1.02-1.06	48
A-20	$D(d,n)He^3$	165	0.46-0.50	5	3.07-3.13	28
A-21	$D(d,n)He^3$	26	2.00-2.02	4	4.9	88
A-23	$T(d,n)He^4$	11	0.26-0.30	1.8	15.2	19

Table II. Track data from nuclear emulsions.

Film no.	ℓ_m (μm)	n	Track density (10^{-6} cm^{-3}) Measured ρ_m	Corrected ρ_t	Expected ρ	N_m total	N_t/N_m $0-\ell_m$	$N^{30\ deg}$	f
A-15	6	1.41	2.8	5.1	5.6	1038	1.80	555	0.65
A-16	11	1.45	2.55	3.5	3.4	2097	1.36	919	0.45
A-18	15	1.48	3.9	5.6	6.4	2868	1.43	1015	0.45
A-20	78	1.56	2.2	2.3	2.0	1591	1.03	483	0.70
A-21	170	1.58	4.5	4.1	4.6	2620	0.905	723	0.79
A-23	1120	1.63	2.0	0.50	0.42	1149	0.250	326	0.97

List of Symbols

θ	Polar half-angle of scattering, i.e., angle between proton track and axis of incident neutron.
Ω	Solid angle defined by $2\pi\ (1-\cos\theta)$.
N, dN, N_0	Number, differential number, and total number of scattering events.
ℓ, ℓ_n, E_p	Track length, maximum track length, and recoil energy of the proton.
E_n	Energy of incident neutrons.
a	A constant; the value is 13.92.
n	A parameter, defined by $l = a\,E_p^n$, normally considered constant; however, it varies slowly with E_p and is given to within 2% from 0.8 to 20 MeV by $0.1\,(E_p)^{1/3}+1.38$.
N_m	Total number of measured tracks in a sample.
$N_m^{30\ \mathrm{deg}}$	Number of measured tracks with $\theta \leq 30$ deg.
N_t	True total number of measured tracks, corrected to exclude stray or second-scattering tracks, and to include the short tracks lost because of scanning inefficiency; given by $(dN/d\ell)_m \cdot n\,\ell_m$.
ρ_m	Measured track density.
ρ	Track density expected; given by product of macroscopic cross section for hydrogen in standard nuclear emulsion and the neutron exposure.
ρ_t	True total measured track density, given by $\rho_m \cdot N_t/N_m$.
f	Fraction of tracks of $l > 0.6\,\ell_m$ with $\theta \leq 30$ deg.

σ	Total cross section for scattering of hydrogen nuclei by neutrons of a given energy.
P	Track-escape probability based on emulsion dimensions and track length.
ΔE	Energy interval.
Δy	Projection of the track length along the axis of the incident neutron.

FIGURE CAPTIONS

Fig. 1. Emulsion holder for edge-normal exposure.

Fig. 2. Differential track-length distribution from single-energy neutron exposure. Ordinate in units of N_0/ℓ_m. Solid line, n = 1.62 (ℓ_m = 1000 μm); dashed line, n = 1.53 (ℓ_m = 40 μm).

Fig. 3. Track-length distribution in nuclear emulsion A-15: ——— expected; ●, full sample; □, 30-deg fraction.

Fig. 4. Track-length distribution in nuclear emulsion A-16: ——— expected; ●, full sample; □, 30-deg fraction.

Fig. 5. Track-length distribution in nuclear emulsion A-18: ——— expected; ●, full sample; □, 30-deg fraction.

Fig. 6. Track-length distribution in nuclear emulsion A-20: ——— expected; ●, full sample; □, 30-deg fraction.

Fig. 7. Track-length distribution in nuclear emulsion A-21: ——— expected; ●, full sample □, 30-deg fraction.

Fig. 8. Track-length distribution in nuclear emulsion A-23: ——— expected; ●, full sample; □, 30-deg fraction; spurious peaks due to α particles are indicated by 1, 2, 3.

Fig. 9. Angular distribution of accepted tracks in A-15: ——— expected; □, xy plane; ●, zy plane.

Fig. 10. Angular distribution of accepted tracks in A-16: ——— expected; □, xy plane; ●, zy plane.

Fig. 11. Angular distribution of accepted tracks in A-18: ——— expected; □, xy plane; ●, zy plane.

Fig. 12. Angular distribution of accepted tracks in A-20: ——— expected; □, xy plane; ●, zy plane.

Fig. 13. Angular distribution of accepted tracks in A-21: ——— expected; □, xy plane; O, zy plane.

Fig. 14. Angular distribution of accepted tracks in A-23: ——— expected; □, xy plane; O, zy plane.

Fig. 15. Neutron energy spectrum in nuclear emulsion A-15; ——— by differentiation of smoothed proton energy spectrum; —.—. from 30-deg fraction, track by track (RECOIL II); energy spread expected (see Table I)

Fig. 16. Neutron energy spectrum in nuclear emulsion A-16: ——— by differentiation of proton energy spectrum; —.—. from 30-deg fraction, track by track (RECOIL II).

Fig. 17. Neutron energy spectrum in nuclear emulsion A-18: ——— by differentiation of proton energy spectrum; —.—. from 30-deg fraction, track by track (RECOIL II).

Fig. 18. Neutron energy spectrum in nuclear emulsion A-20: ——— by differentiation of proton energy spectrum; —.—. from 30-deg fraction, track by track (RECOIL II).

Fig. 19. Neutron energy spectrum in nuclear emulsion A-21: ——— by differentiation of proton energy spectrum; —.—. from 30-deg fraction, track by track (RECOIL II).

Fig. 20. Neutron energy spectrum in nuclear emulsion A-23: ——— by differentiation of smoothed proton energy spectrum; —.—. from 30-deg fraction, track by track (RECOIL II); 1, 2, 3: spurious peaks due to α particles.

Fig. 21. Macroscopic cross sections for neutron interactions in nuclear emulsion: I, total; II, elastic scattering; III, hydrogen; IV, n, n'; V, n, n' plus n, 2n; R, ratio of III to II. For I, II, IV, V the ordinate is the sum of the macroscopic cross sections of Ag, Br, H, C, O, and N.

Fig. 22. Three-axis digitized microscope.

Fig. 23. Block diagram of electronic apparatus associated with the three-axis digitized microscope.

M_x Mechanical coupling to shaft of precision lead screw which moves microscope stage along the x axis.

E_x Encoder which senses shaft-rotation position of x-axis lead screw.

C_x Control chassis which converts binary code of encoder to decimal.

M_y, E_y, C_y, and M_z, E_z, C_z refer to similar y- and z-axis elements.

F Fixed information dial panel.

B Button for punch circuit activation.

PC Card-punch control.

P Card-punch machine.

R Relay bank and power supply.

Fig. 24. Semiautomatic track-scanning apparatus.

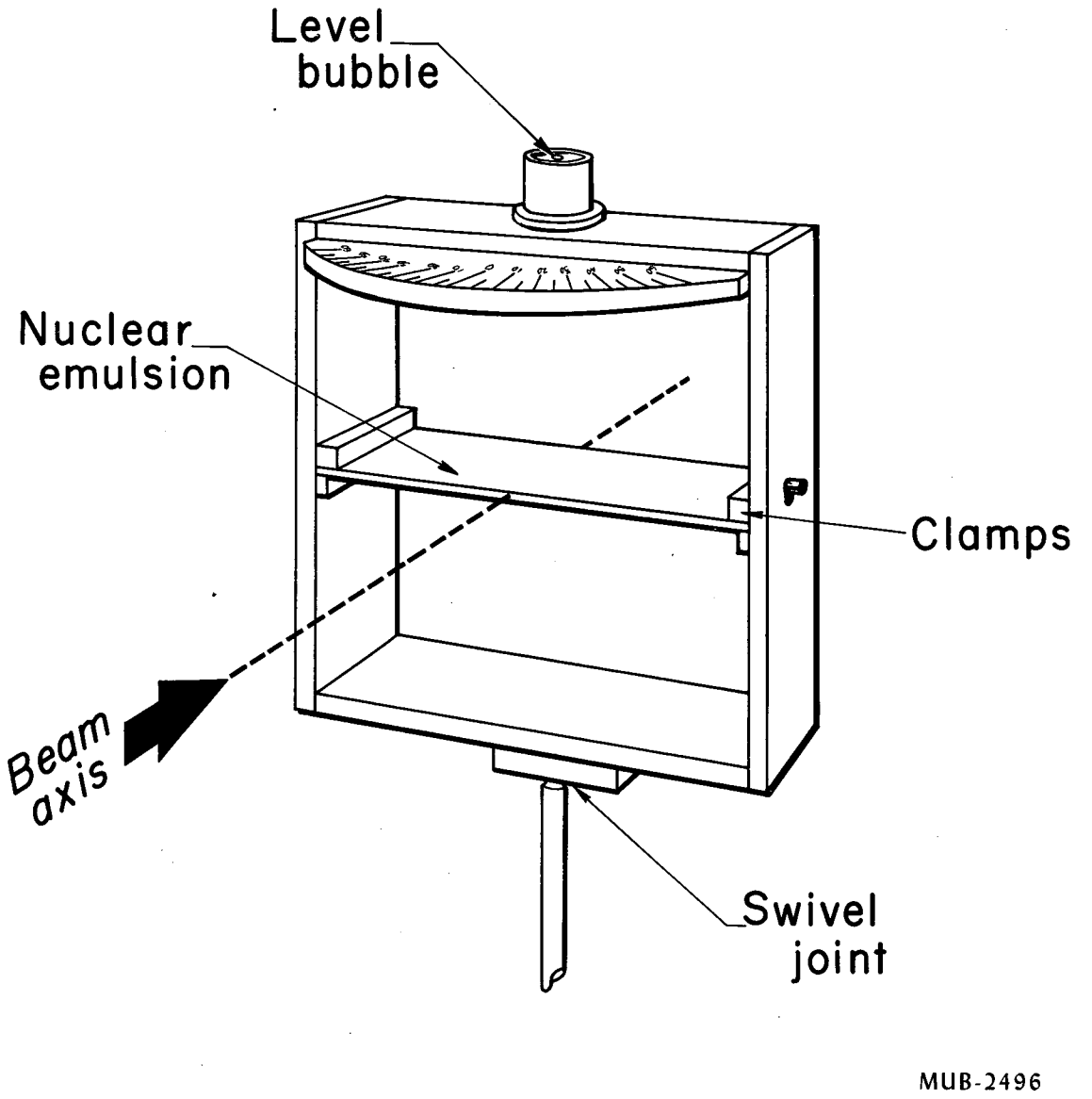
Level bubble
Nuclear emulsion
Clamps
Beam axis
Swivel joint
MUB-2496

Fig. 1

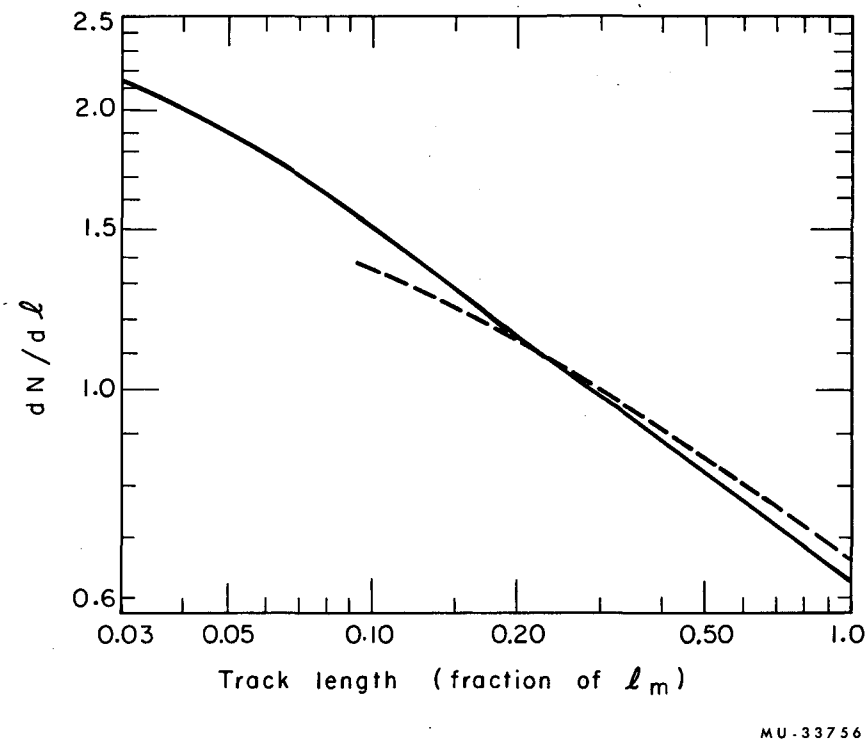
2.5
2.0
1.5
1.0
0.6
dN/dℓ
0.03
0.05
0.10
0.20
0.50
1.0
Track length (fraction of ℓm)
MU-33756

Fig. 2

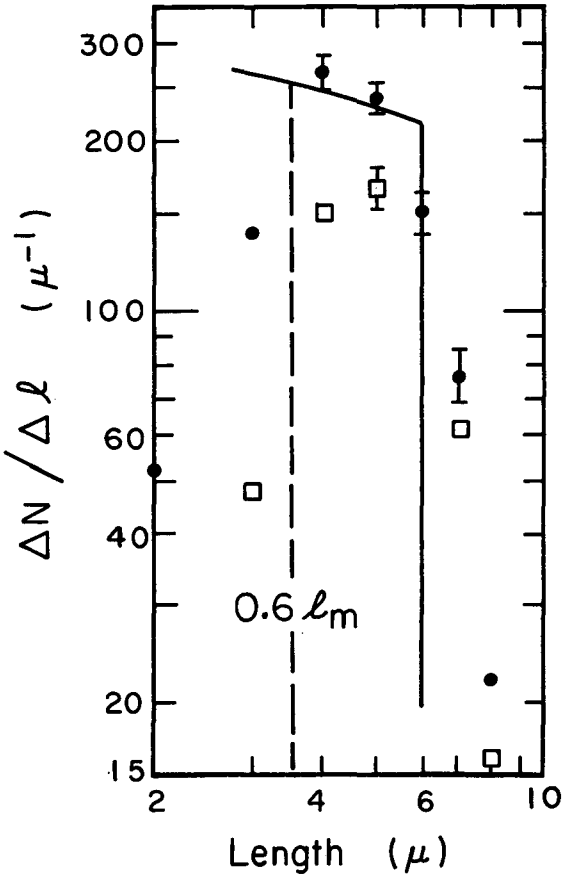

MU-33757

Fig. 3

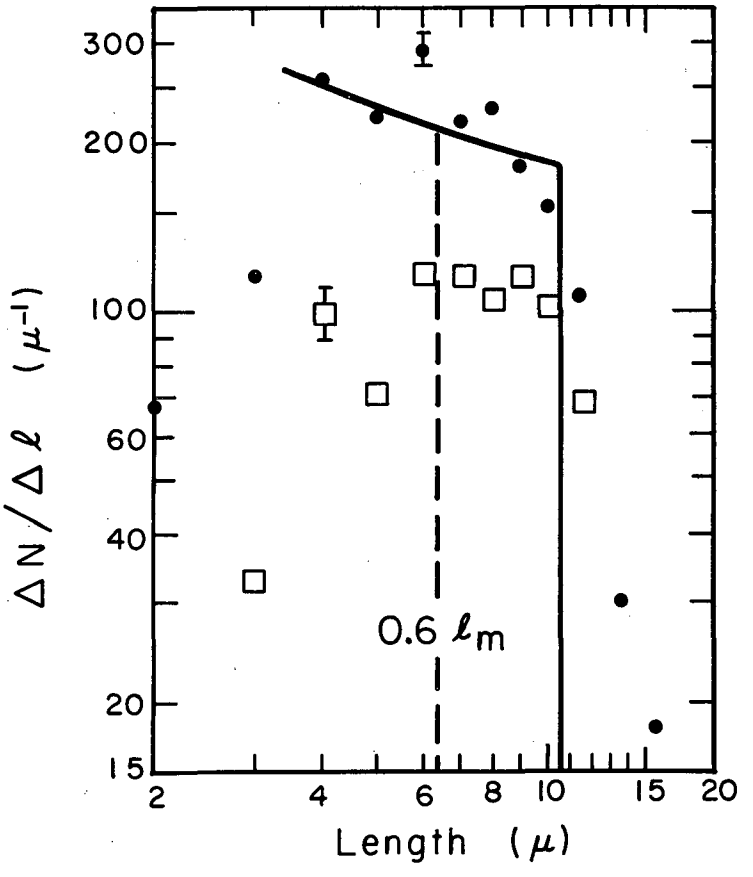

MU-33758

Fig. 4

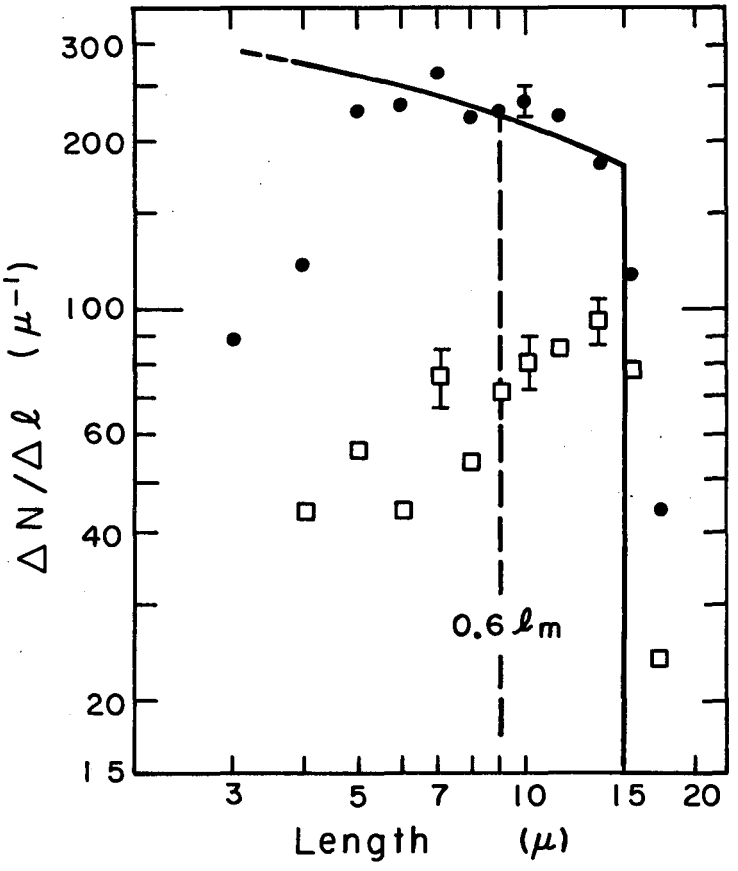

MU-33759

Fig. 5

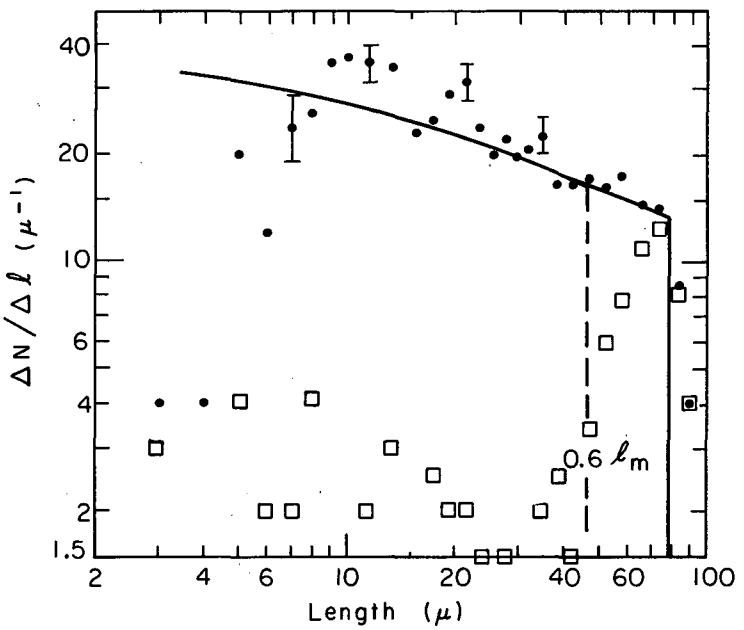

MU-33760

Fig. 6

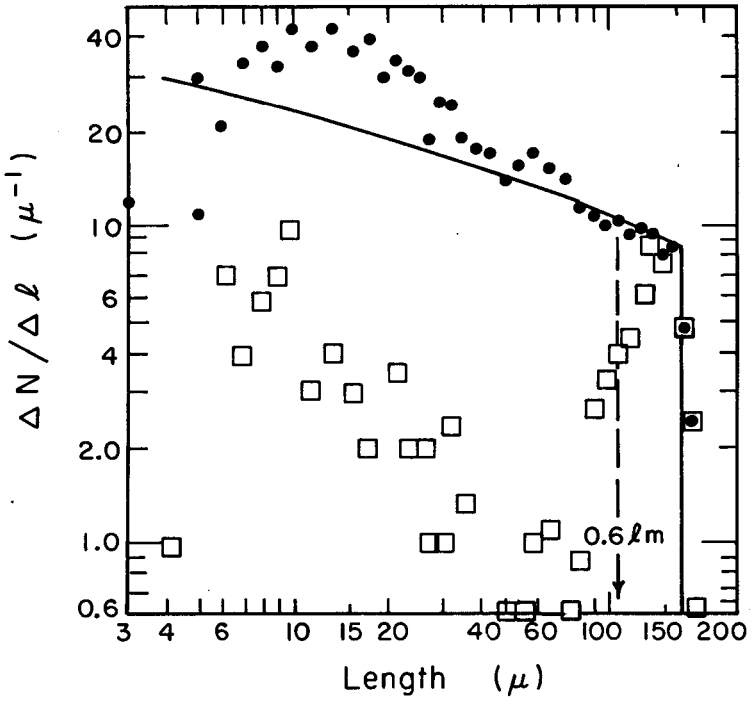

MU-33776

Fig. 7

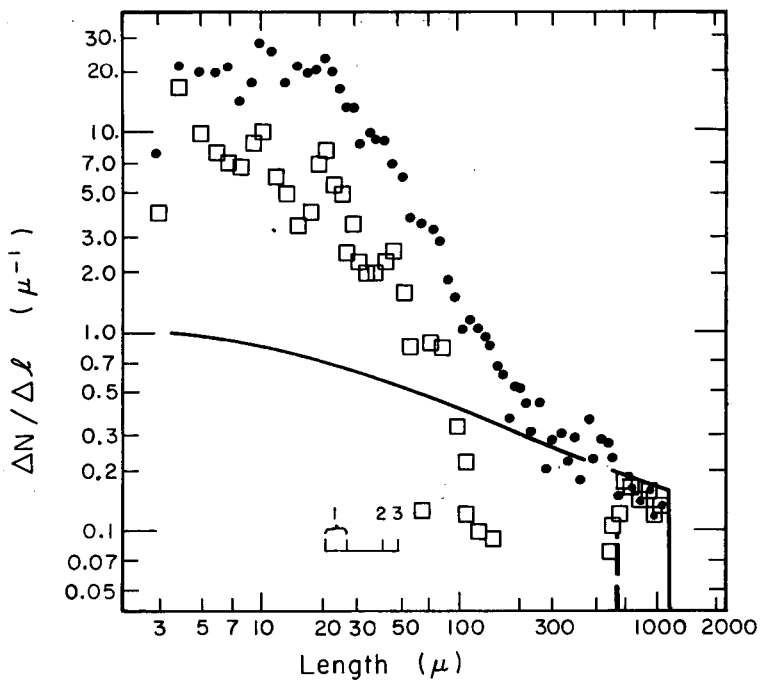

MU-33761

Fig. 8

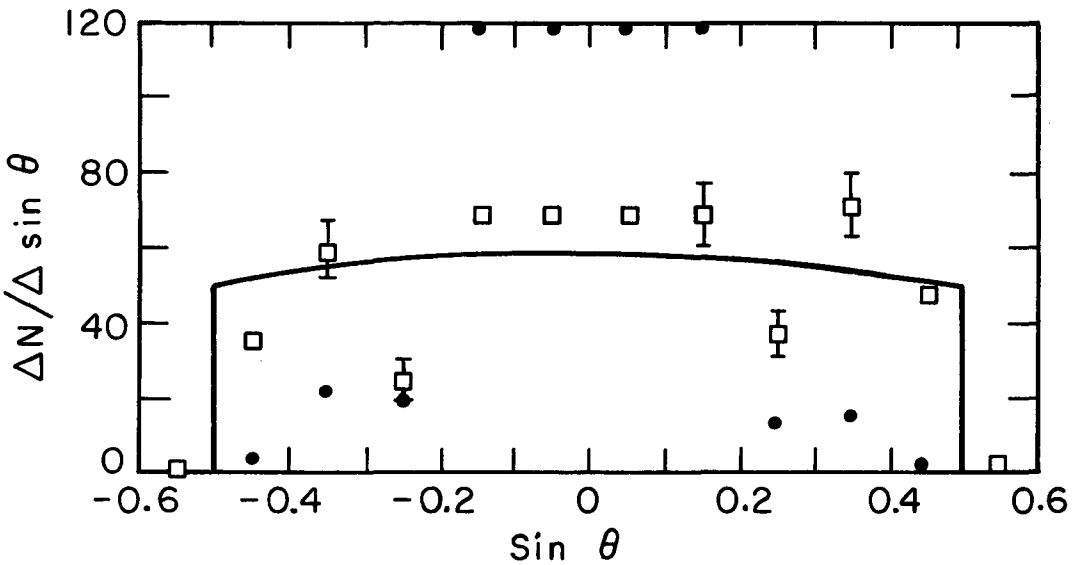

MU-33762

Fig. 9

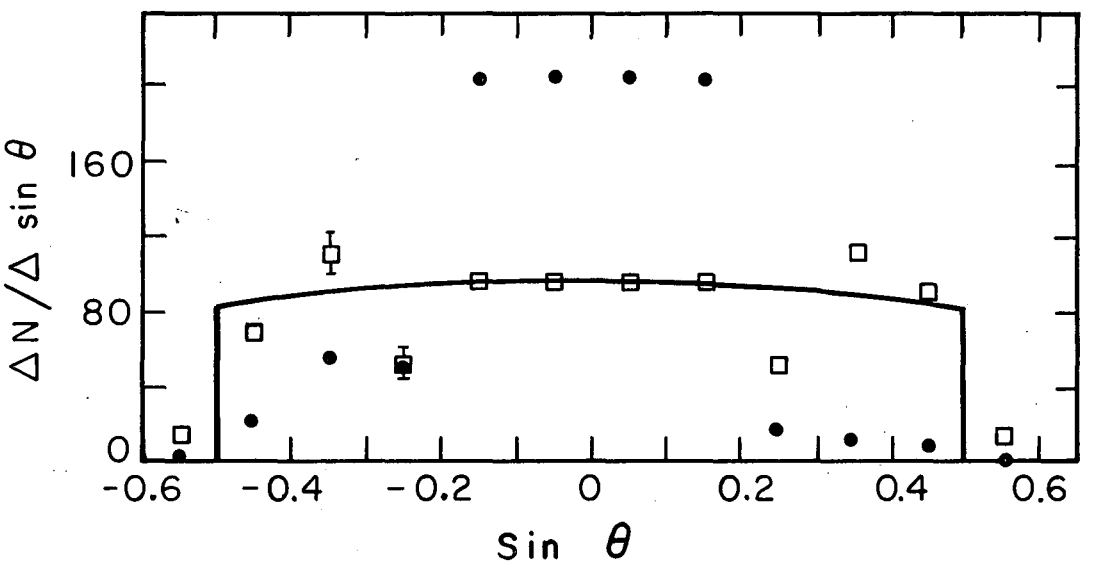

MU-33763

Fig. 10

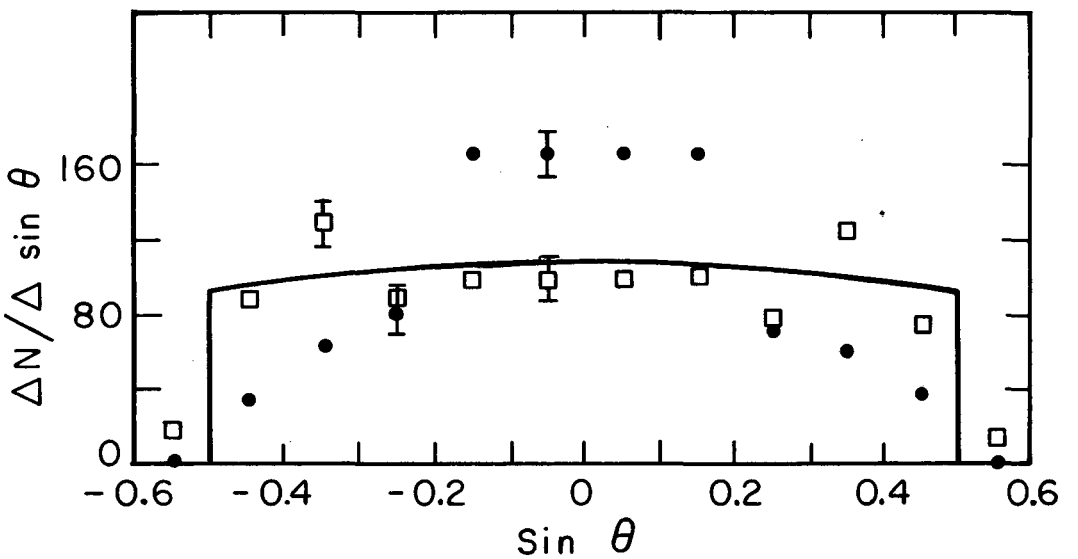

MU-33764

Fig. 11

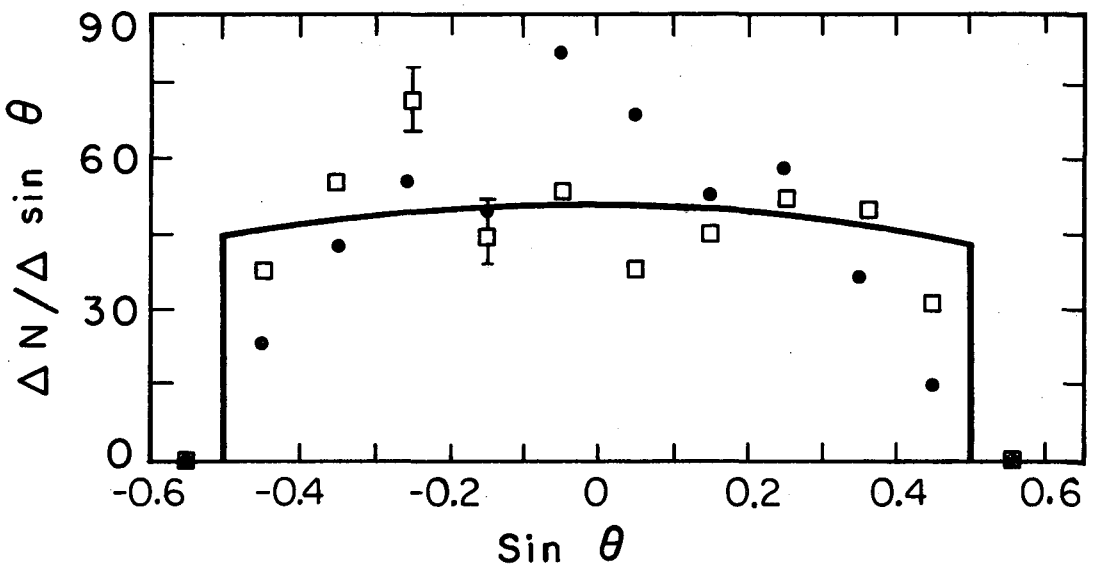

MU-33766

Fig. 12

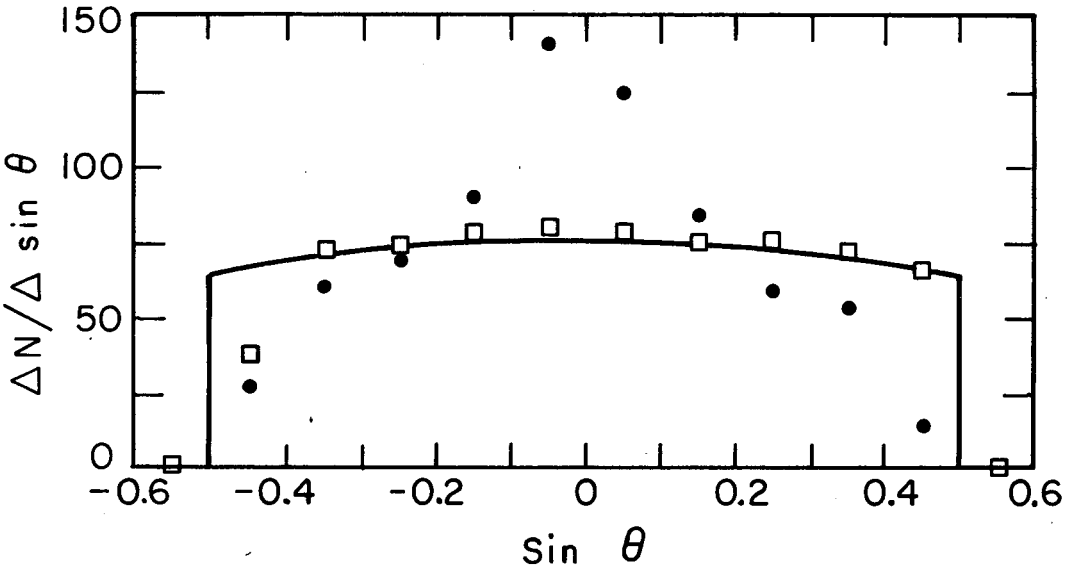

MU-33765

Fig. 13

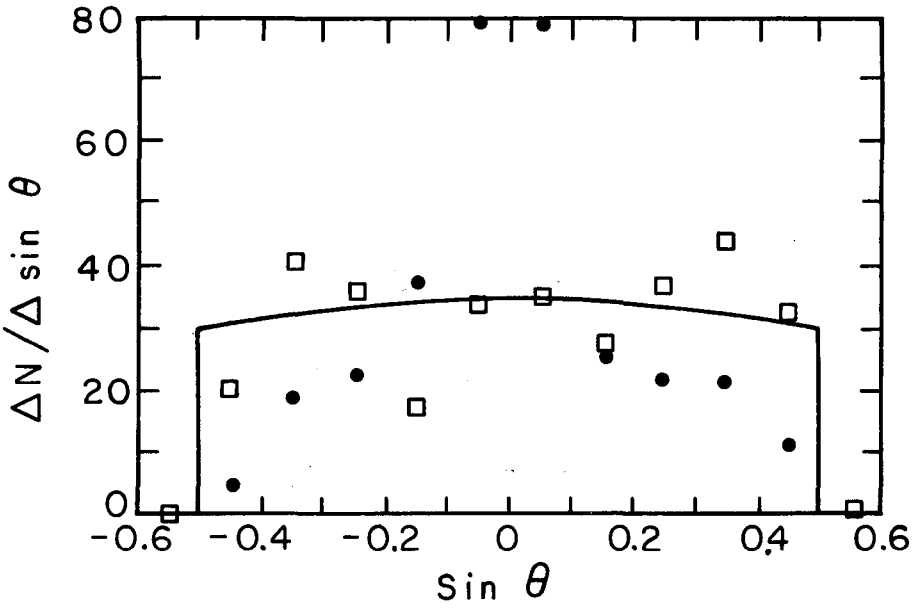

MU-33767

Fig. 14

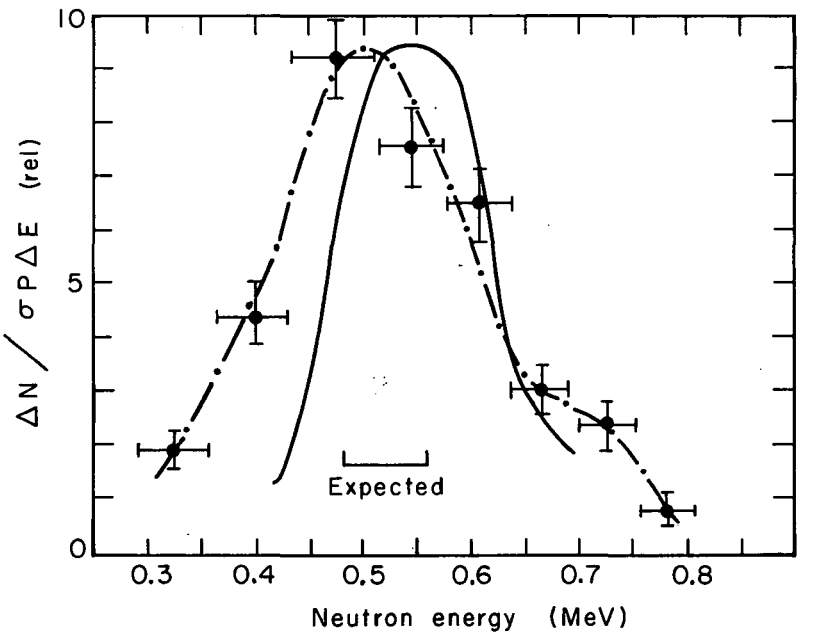

MU-33769

Fig. 15

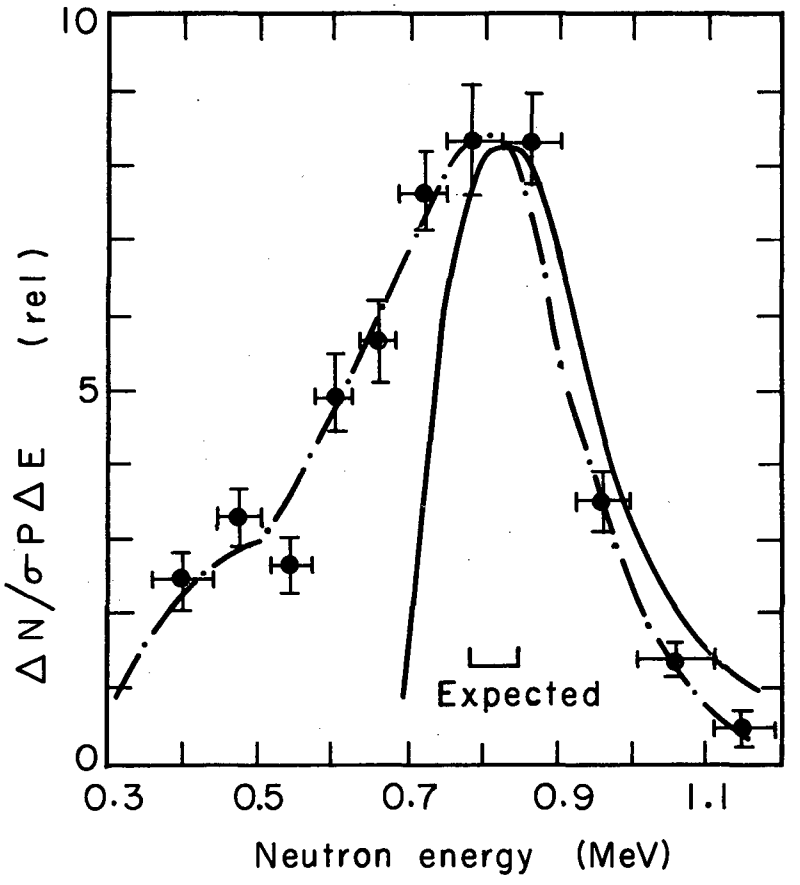

MU-33771

Fig. 16

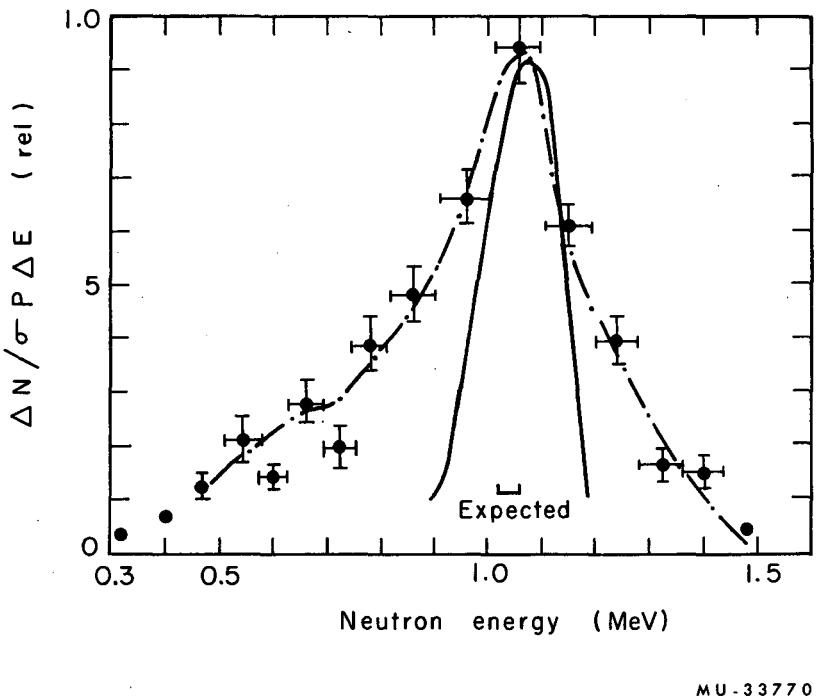
1.0
5
0
ΔN/σPΔE (rel)
0.3
0.5
1.0
1.5
Neutron energy (MeV)
Expected
MU-33770

Fig. 17

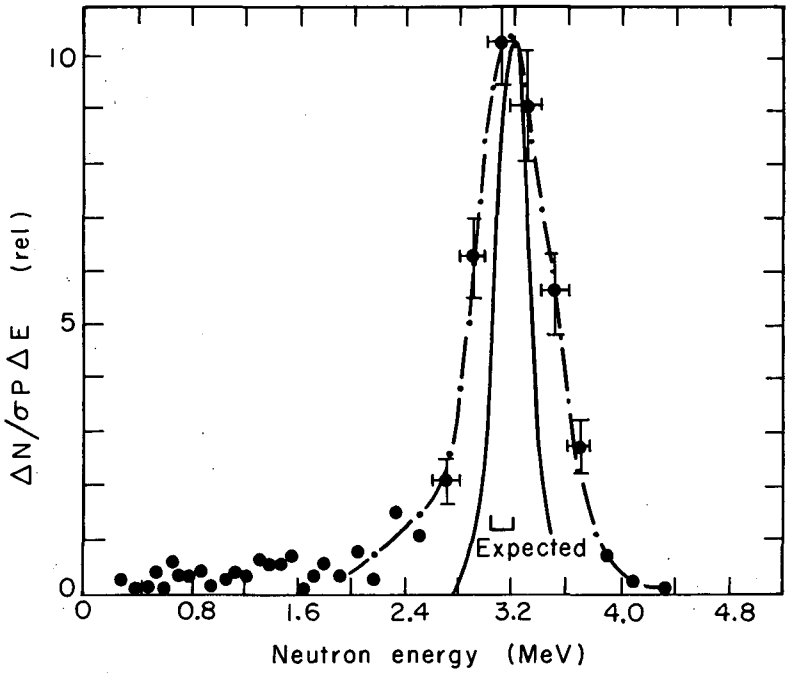

MU-33772

Fig. 18

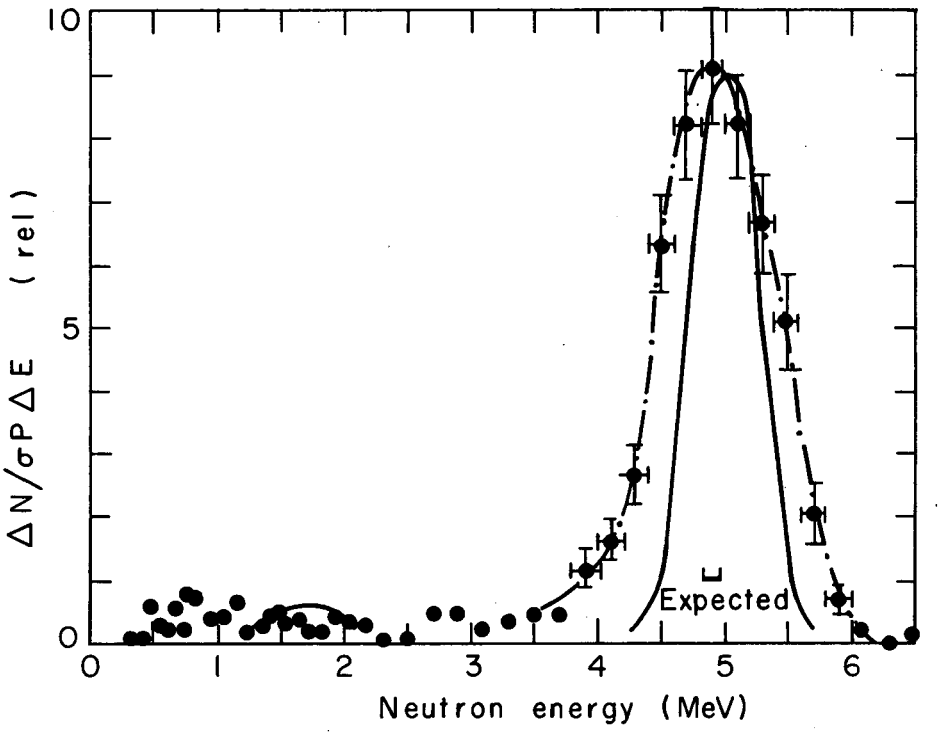

MU-33773

Fig. 19

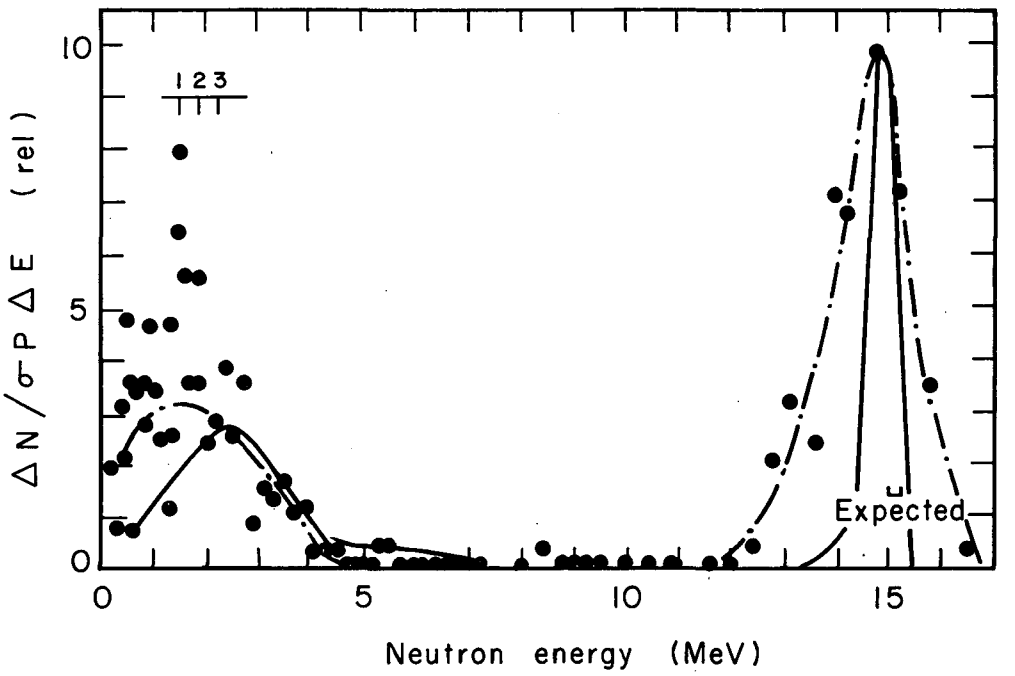

MU-33768

Fig. 20

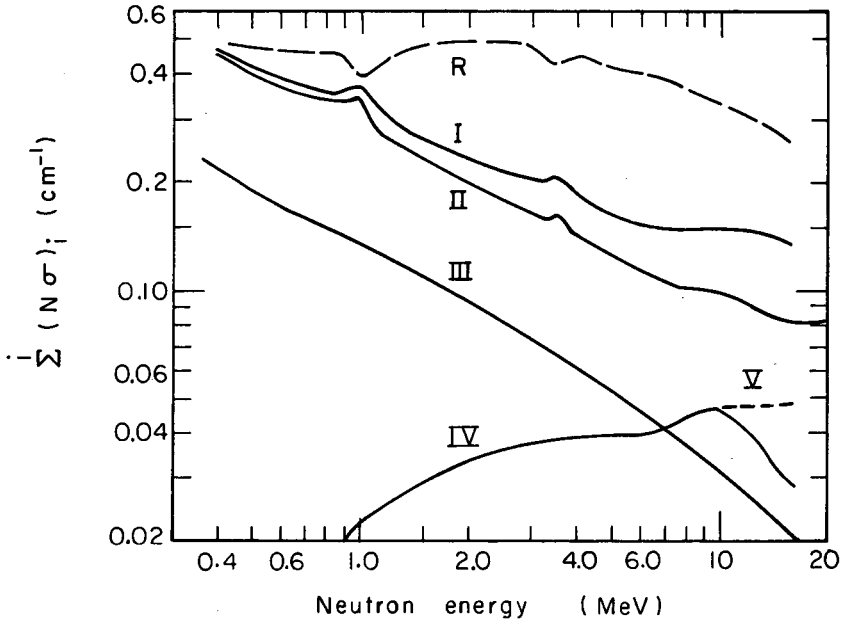

MU-33774

Fig. 21

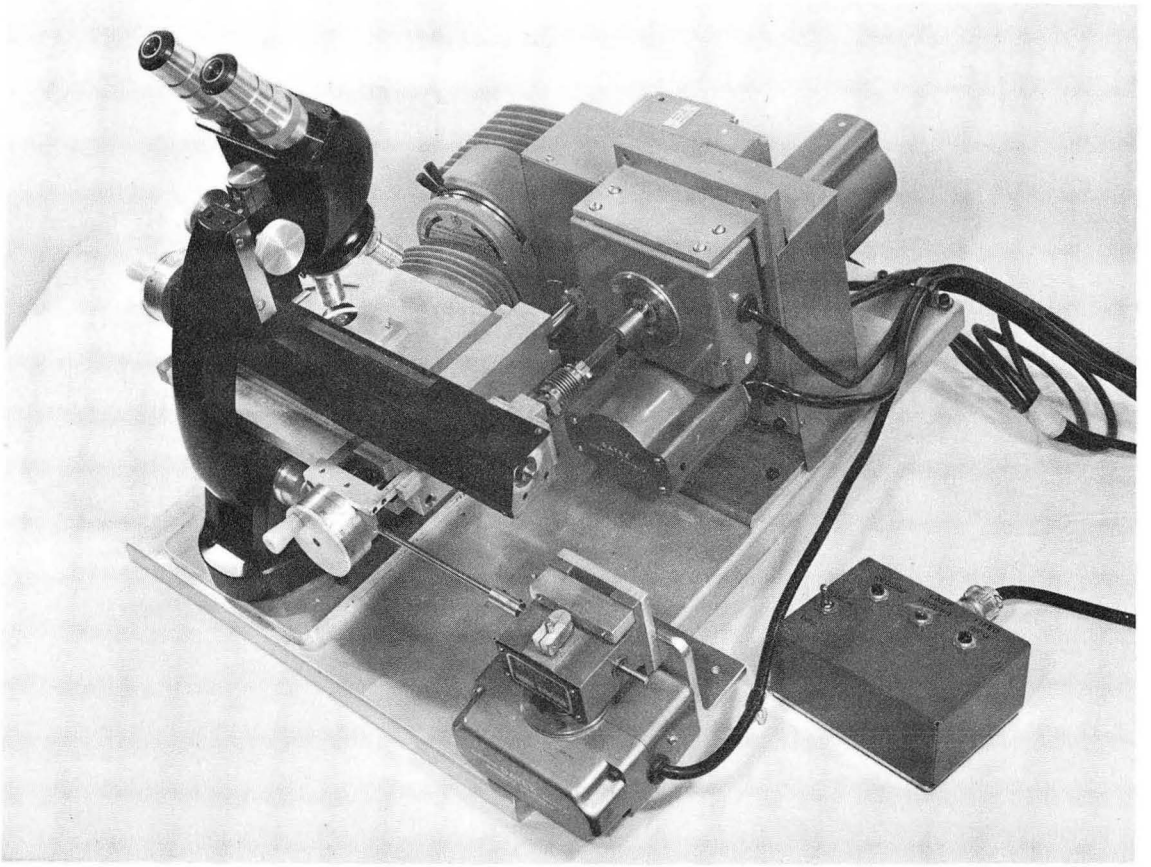

ZN-4233

Fig. 22

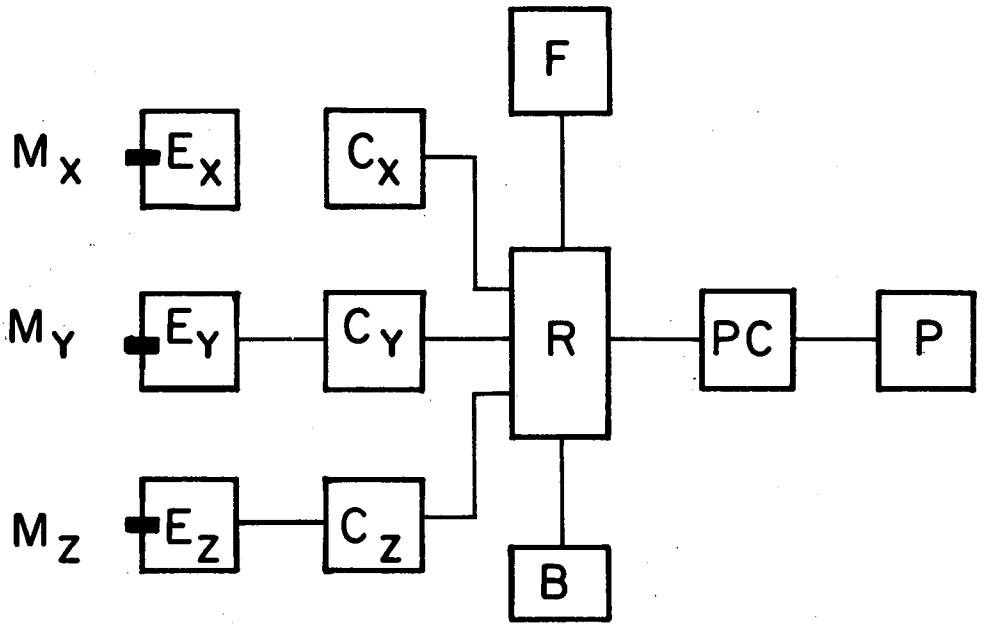

MU-33775

Fig. 23

ZN-4234

Fig. 24

This report was prepared as an account of Government sponsored work. Neither the United States, nor the Commission, nor any person acting on behalf of the Commission:

A. Makes any warranty or representation, expressed or implied, with respect to the accuracy, completeness, or usefulness of the information contained in this report, or that the use of any information, apparatus, method, or process disclosed in this report may not infringe privately owned rights; or

B. Assumes any liabilities with respect to the use of, or for damages resulting from the use of any information, apparatus, method, or process disclosed in this report.

As used in the above, "person acting on behalf of the Commission" includes any employee or contractor of the Commission, or employee of such contractor, to the extent that such employee or contractor of the Commission, or employee of such contractor prepares, disseminates, or provides access to, any information pursuant to his employment or contract with the Commission, or his employment with such contractor.